CHEMICAL & PHARMACEUTICAL BULLETIN

Vol. 31, No. 1 January 1983

Regular Articles

[Chem. Pharm. Bull. 31(1) 1—11 (1983)]

Application of a Membrane Reactor to Gas–Liquid Two-phase Enzyme Reactions: Oxidation of Glucose by Soluble Immobilized Glucose Oxidase and Catalase[1)]

MORIFUMI HASHIMOTO, TOYOHISA TSUKAMOTO, SHUSHI MORITA, and JUTARO OKADA*

Faculty of Pharmaceutical Sciences, Kyoto University, Yoshida-Shimoadachi-cho Sakyo-ku, Kyoto 606, Japan

(Received June 23, 1982)

The oxidation of glucose to gluconic acid was carried out at 20°C in a membrane reactor in which a solution of glucose oxidase (EC 1.1.3.4) and catalase (EC 1.11.1.6) was entrapped between two semipermeable membranes of regenerated cellulose. A buffered solution (pH 5.5) of glucose saturated with oxygen was fed continuously through one grooved compartment outside the membranes (liquid side), and oxygen gas was supplied at a pressure slightly higher than 1 atm to the opposite grooved compartment (gas side).

First, by holding one sheet of membrane between the two sides, experiments were performed to determine the membrane permeation coefficient for oxygen in the liquid (k_M) and the liquid-to-membrane mass transfer coefficient for oxygen in the liquid (k_L). The value of k_M was proportional to the difference between the gas- and liquid-side pressures and the value of k_L was proportional to the 0.56th power of the liquid flow rate.

The reaction studies were done under conditions where the transfer of oxygen was a key process. From individual measurements of the absorption (permeation) rates of oxygen in the liquid through both membranes, it was found that, at low liquid flow rate, the transfer through the gas-side membrane contributed greatly to the global rate of absorption (reaction). For the mixing of enzyme solution, two models were considered; the stagnant and mixing models. At low liquid flow rate, the rate data were well explained by the stagnant model. At high liquid flow rate, in contrast, the mixing model was applicable. The oxygen pressure and the membrane permeation coefficient were the most important factors affecting the global rate of reaction.

Keywords——membrane reactor; oxidation; glucose; glucose oxidase; catalase; permeation coefficient; regenerated cellulose; mass transfer

The immobilization of enzyme has been extensively studied by numerous investigators, and many reviews and books have been published.[2)] The techniques of immobilization can be conveniently divided into three groups; gel lattice immobilization, adsorption or covalent linkage to supports, and encapsulation.

One of the methods for encapsulation, the entrapment of free enzymes by a semipermeable membrane, offers several advantages for an enzyme reactor. In this type of reactor, the membrane reactor, immobilization of the enzyme can be accomplished easily, so that the reactor activity can be maintained by introducing fresh enzyme and withdrawing deactivated enzyme. Since no chemical modification of the enzyme is necessary, the kinetic properties of enzyme do not alter. Moreover, the membrane reactor can be easily applied to multi-enzyme

and/or multi-substrate reactions. Because of these advantages, membrane reactors have been widely used in liquid-phase enzyme reactions.[3,4] It has been shown that the rate of reaction is reduced by the resistances of substrate transfer from the bulk liquid to the membrane surface and of substrate permeation through the membrane.[4]

There are a number of important enzyme reactions involving both gas and liquid phase substrates. However, the application of a membrane reactor to such a system has not yet been reported. For such a reaction system, the gas phase substrate is expected to be a limiting reactant, because the solubility of gas in the liquid is usually low. Therefore, a means of increasing the mass transfer of gaseous substrate is required for the effective use of the enzyme activity. Similar considerations apply to a trickle-bed reactor packed with immobilized enzyme particles.[5]

We designed a new type of membrane reactor for gas–liquid two-phase enzyme reactions. In order to investigate its applicability, the oxidation of glucose to gluconic acid by glucose oxidase and catalase was selected as a model reaction. The reaction kinetics is well known and the intrinsic rate of reaction is quite high.[6,7] The solution of enzymes was entrapped between two semipermeable membrane sheets. The glucose solution was fed through one compartment outside the membranes and oxygen gas was supplied to the other compartment. With this configuration, the global rate of reaction depended on the absorption(permeation) rates of oxygen through both membranes.

Experimental

Chemicals——Glucose oxidase (EC 1.1.3.4, from *Aspergillus niger*, 17300 units/g stated activity) and catalase (EC 1.11.1.6, from bovine liver, 2100 units/mg stated activity) were both purchased from Sigma Chemical Co. Commercial oxygen and nitrogen gases were used without further purification. All other reagents were purchased from Wako Pure Chemical Industries, Ltd.

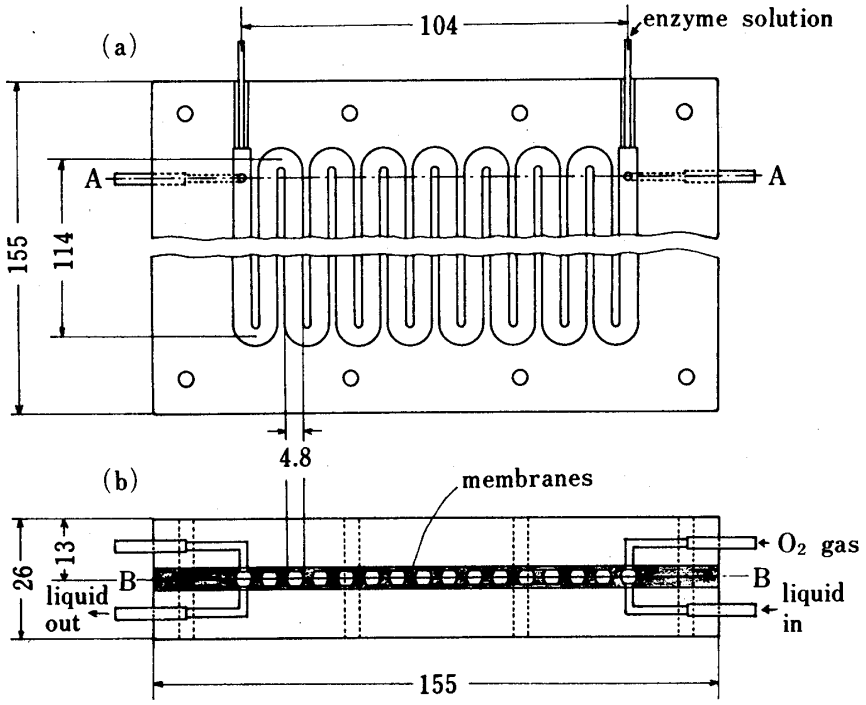

Fig. 1. Details of the Membrane Reactor
(a), horizonal sectional view taken on line B—B in(b); (b), vertical sectional view taken on line A—A in (a); dimensions in mm.

Apparatus and Operating Procedure——(a) Reaction Experiments: The membrane reactor used is illustrated in Fig. 1. For our experimental purposes, a Zeineh dialyzer (model D-1, Biomed Instruments) was modified by cutting the connections of the upper and lower paths, and two additional tubes were attached to the module. Two sheets of regenerated cellulose membrane (Biomed Instruments) were held between two

acrylate plates having a long zig-zag groove in the interior side of the plate. A 10 ml aliquot of enzyme solution (in 0.1 M acetate buffer, pH 5.5) containing 20 mg of glucose oxidase and 20 mg of catalase was entrapped between the two semipermeable membranes. The reactor as a whole thus consisted of three sections, a liquid-side section where the glucose solution was flowing, a gas-side section to which oxygen gas was supplied and a section containing entrapped enzyme solution. Note that catalase was used to decompose hydrogen peroxide formed by the reaction between glucose and oxygen. The reactor dimensions and the physical properties of the membrane are summarized in Table I.

TABLE I. Reactor Dimensions and Physical Properties of the Membrane

Reactor:	
Length of the groove, cm	178.8[a]
Cross section of the groove (symmetric trapezoid), cm	0.48[a](Lower base) 0.32[a](Upper base) 0.20[a](Height)
Thickness of the enzyme solution, cm	0.117[b]
Membrane:	
Thickness, nm	20[a]
Pore size, Å	15[c]
Molecular weight cut-off	7000[c]

a) Measured.
b) Calculated from the volume of enzyme solution added.
c) From Biomed Instruments.

Figure 2 shows a schematic diagram of the apparatus used. First, in a reservoir 2, 0.1 M glucose solution (in 0.1 M acetate buffer, pH 5.5) was saturated with oxygen. The solution was introduced into the lower compartment (liquid side) of the membrane reactor 1 by means of the tube pump 3, and circulated through the reactor system. The inlet and outlet pressures of the liquid and the liquid flow rate were measured with manometers 4 and a rotameter 5, respectively. The glucose solution in the reservoir was kept saturated by bubbling oxygen gas through it. The oxygen gas was circulated by means of a pump 7 as shown in Fig. 2. Oxygen gas was applied to the other compartment (gas side) of the reactor at a pressure slightly higher than 1 atm. The gas pressure was measured from the difference between the two liquid levels. In the steady state, the amounts of oxygen that permeated through gas- and liquid-side membranes were measured by means of the gas burettes 6 and 8, respectively. The number of moles of oxygen was evaluated from the gas law. The reactor and reservoir were contained in a constant temperature bath at 20°C. The experimental conditions are summarized in Table II.

TABLE II. Experimental Conditions and Physical Properties of the Glucose Solution

Permeation experiment:	
Concentration of glucose in the liquid, C_S, mol/cm^3	1.0×10^{-4}
Liquid flow rate, Q_L, cm^3/s	0.095—1.11
Liquid pressure at the reactor inlet, $(P_L)_{in}$, atm	1.00—1.27
Gas pressure applied, P_G, atm	1.00—1.22
Temperature, °C	20
Reaction experiment:	
Concentration of glucose in the liquid, C_S mol/cm^3	1.0×10^{-4}
Concentration of glucose oxidase, C_E, unit/cm^3	34.6
Concentration of catalase, unit/cm^3	4200
Volume of the enzyme solution, cm^3	10
Liquid flow rate, Q_L, cm^3/s	0.090—1.02
Liquid pressure at the reactor inlet, $(p_L)_{in}$, atm	1.00—1.20
Gas pressure applied, p_G, atm	1.00—1.15
Temperature, °C	20
Physical properties of the glucose solution:	
Density, g/cm^3	1.0[a]
Viscosity, g·cm/s	1.0×10^{-2} [a]
Solubiliy of oxygen in the liquid at 20°C, 1 atm, mol/cm^3	1.36×10^{-6} [a]
Diffusivity of oxygen in the liquid at 20°C, D_L, cm^2/s	2.0×10^{-5} [b]

a) Measured.
b) Assumed to be identical with that in water at 20°C.[11]

(b) Permeation Experiments: Prior to the reaction studies, permeation experiments were done to determine the membrane permeation coefficient for oxygen in the liquid and the liquid-to-membrane mass transfer coefficient for oxygen in the liquid. A sheet of membrane was held in the same reactor as shown in Fig. 1. Several changes in the apparatus shown in Fig. 2 were made; (1) a heater was fitted to the reservoir 2, (2) a cooling tube was introduced into the feed line and immersed in the constant temperature bath, and (3) the pump 7 and the gas burette 8 were removed. Nitrogen gas was bubbled through the boiling 0.1 M glucose solution in the reservoir. After passing through the cooling tube, the degassed solution was introduced into the liquid side of the reactor, and the effluent was returned to the reservoir. Oxygen gas was supplied to the gas side of the reactor. During this operation, the concentration of oxygen in the glucose solution in the reservoir was always less than 0.5% saturation. This was checked by means of an oxygen analyzer (Toshiba-Beckman, Model 777). Other details were the same as for the reaction experiments. The experimental conditions are also summarized in Table II.

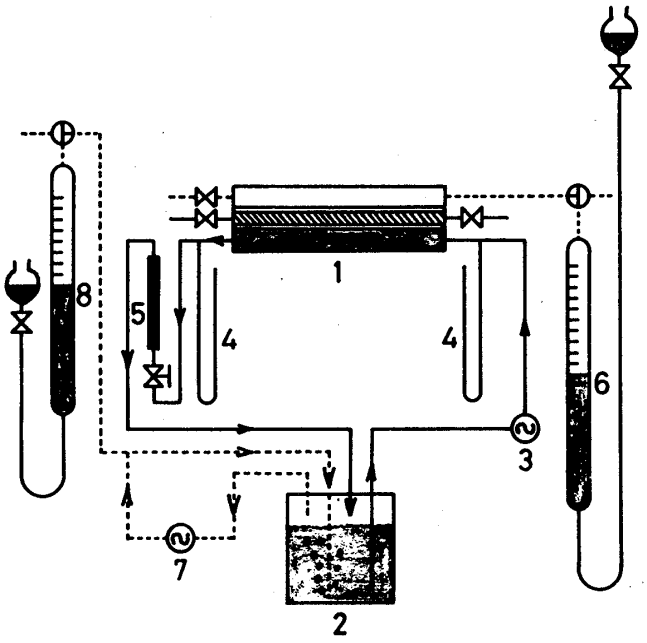

Fig. 2. Schematic Diagram of the Apparatus used for the Reaction Experiment

⟶, liquid flow line; ---→--, gas flow line; 1, membrane reactor; 2, reservoir; 3, tube pump for liquid; 4, manometer; 5, rotameter; 6, gas burette; 7, gas pump for O_2; 8, gas burette.

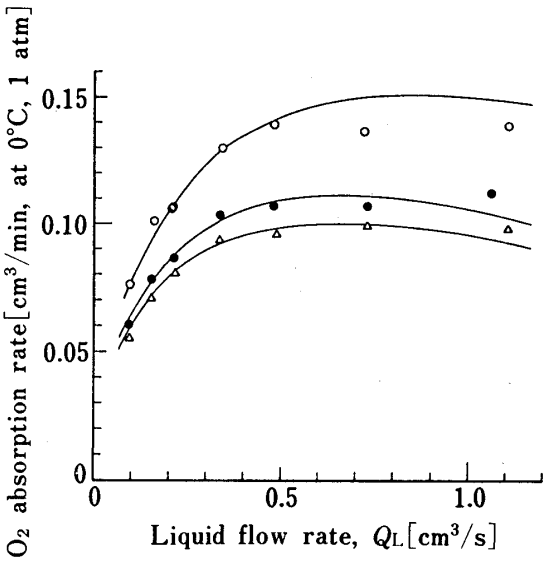

Fig. 3. Effect of Liquid Flow Rate on the Global Rate of Oxygen Absorption

P_G [atm]: ○, 1.14 ; ●, 1.05 ; △, 1.02 ; —, calculated curve.

Results and Discussion

I. Membrane Permeation and Mass Transfer Coefficients

(a) Influence of Liquid Flow Rate and Gas Pressure——Typical results of the permeation experiments are shown in Fig. 3. The global rate of absorption (permeation) for oxygen increases with increase in both the liquid flow rate, Q_L [cm^3/s], and the oxygen pressure applied to the gas-side compartment, p_G [atm]. This means that the mass transfer of oxygen from the bulk liquid to the membrane surface, as well as the dependence of the membrane permeation coefficient on the pressure difference between the gas and liquid sides, must be taken into consideration.

(b) Theoretical Development——The groove in the reactor is assumed to be straight, though in fact it has a zig-zag structure as shown in Fig. 1(a). In the steady state, the concentration of oxygen in the bulk liquid, C_L [mol/cm^3], can be expressed by the following mass balance equation;

$$Q_L \frac{dC_L}{dz} = k_M a(C_G - C_M) = k_L a(C_M - C_L) \qquad (1)$$

where z [cm] is the axial distance from the reactor inlet, k_M [cm/s] and k_L [cm/s] are the membarne permeation coefficient and the liquid-to-membrane mass transfer coefficient, respectively, a [cm] is the surface area per unit axial length, that is, the width of the membrane in the groove, and C_G [mol/cm^3] and C_M [mol/cm^3] are the concentrations of oxygen in the liquid at the membrane surfaces of the gas side and of the liquid side, respectively.

C_G can be assumed to be the saturated concentration, so that

$$C_G = p_G/H \tag{2}$$

where H[atm·cm^3/mol] is Henry's constant. This assumption is reasonable, because there is no flowing liquid on the gas-side membrane surface, and because the oxygen gas is in direct contact with the liquid near the pore mouths at the surface.

The membrane permeation coefficient is assumed to be linearly related to the difference between p_G and the liquid pressure, p_L [atm].

$$k_M = (k_M)_0 + k_P(p_G - p_L) \tag{3}$$

where k_P [cm/(s·atm)] is the proportionality constant and $(k_M)_0$ [cm/s] is the membrane permeation coefficient at $p_G = p_L$. Equation (3) is reasonable when the membrane is located between two liquid phases and an ultrafiltration flux exists through the membrane.[8] This is not the case for the present reactor, as there is no liquid flow inside the pores. However, an increase in $(p_G - p_L)$ results in a decrease in the length of the diffusion path, which means an increase in k_M. Though the linear relationship between k_M and $(p_G - p_L)$ is not well understood, the inherent error may be small because the absolute value of $(p_G - p_L)$ is not large under our experimental conditions.

Since the decrease in the liquid pressure (due to the friction force) should be proportional to the distance z, p_L can be given by

$$p_L = (p_L)_{in} - \{(p_L)_{in} - (p_L)_{out}\} z/z_t \tag{4}$$

The boundary conditions for eq. (1) are

$$C_L = 0,\ p_L = (p_L)_{in} \qquad \text{at } z = 0 \tag{5}$$

$$C_L = (C_L)_{out},\ p_L = (p_L)_{out} \qquad \text{at } z = z_t \tag{6}$$

where z_t [cm] is the total length of the groove and the subscripts in and out mean the inlet and outlet of the reactor.

Using eqs. (2) to (6), eq. (1) can be integrated to give

$$K = \frac{Q_L}{az_t} \ln \frac{(p_G/H)}{(p_G/H) - (C_L)_{out}} = k_L - \frac{k_L^2}{k_P B} \ln \left\{ 1 + \frac{k_P B}{k_L + (k_M)_0 + k_P A} \right\} \tag{7}$$

where K is the value obtainable from the experimental data using the second term of eq. (7), A is the pressure difference at the inlet of the reactor between the gas side and the liquid side, and B is the pressure drop in the reactor;

$$A = p_G - (p_L)_{in} \tag{8}$$

$$B = (p_L)_{in} - (p_L)_{out} \tag{9}$$

When Q_L is small, A is nearly zero. Hence, eq. (7) can be expanded in a series for B using the Maclaurin expansion. Ignoring the terms higher than the second power in B gives a linear relationship between K and B;

$$K = \frac{(k_M)_0 k_L}{(k_M)_0 + k_L} + \frac{k_P k_L^2}{2\{(k_M)_0 + k_L\}^2} B \tag{10}$$

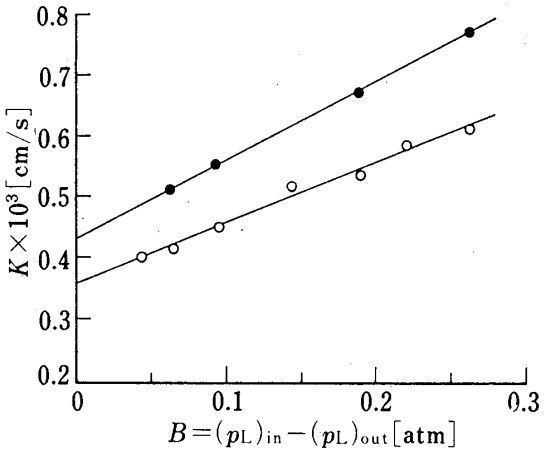

Fig. 4. Relation between K and B at Low Liquid Flow Rate

O_L [cm³/s], A [atm] : ○, 0.095, 3.0×10^{-4} ; ●, 0.156, -4.0×10^{-4}.

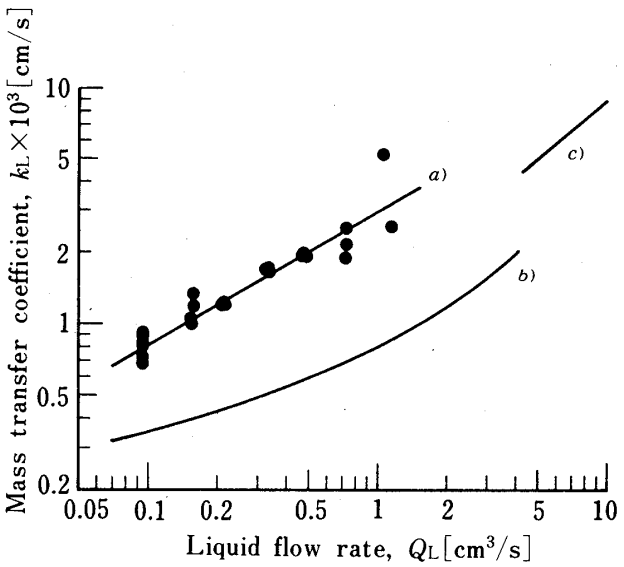

Fig. 5. Liquid-to-Membrane Mass Transfer Coefficient *vs.* Liquid Flow Rate

a) This work. *b*) Sherwood *et al.* (round tube, laminar flow); *c*) Linton *et al.* (round tube, turbulent flow).

Then, if $(k_M)_0$ is known, the value of k_P can be evaluated from the intercept and the slope.

(c) Membrane Permeation Coefficient——First, to determine $(k_M)_0$, a stirred flow dialysis cell was used. The degassed glucose solution was introduced into one chamber in which the liquid was magnetically stirred. Oxygen gas was supplied to the other chamber. This experiment was performed at 20°C in such a way that the pressure of gas and liquid was equal to 1 atm. The absorption (permeation) rate of oxygen was measured without liquid-to-membrane mass transfer limitation; that is, the rate did not depend on the stirring speed. The results gave a value of $(k_M)_0$ of 0.78×10^{-3} [cm/s].

Figure 4 shows plots of K against B (based on eq.(10)) at low liquid flow rates. The lines were estimated by the least-squares method. By using the value of $(k_M)_0$, the value of k_P are obtained as 9.5×10^{-3} and 8.6×10^{-3} [cm/(s·atm)] for $Q_L=0.095$ and 0.156 [cm³/s], respectively. As the obtained values of k_P are nearly equal, the average value of $k_P=9.1\times10^{-3}$ [cm/(s·atm)] was adopted.

(d) Liquid-to-Membrane Mass Transfer Coefficient——The value of k_L can be estimated from eq. (7) by the trial and error method, using the obtained values of $(k_M)_0$ and k_P. The results are shown against Q_L in Fig. 5; the relationship can be described by the following equation.

$$k_L = 3.0\times10^{-3}Q_L^{0.56} \quad [\text{cm/s}] \tag{11}$$

As shown in Fig. 1(b), the cross section of the compartment (perpendicular to the z direction) is a symmetric trapezoid and the solute (oxygen) transfers from the membrane side to the opposite side. No suitable correlation (or analytical solution) for k_L seems to have been presented in the literature for such a configuration, so the obtained values of k_L were compared with those for a round tube. Assuming the cross section to be circular, the Reynolds numbers, Re [−], are in the range of 38 to 440 under our experimental conditions. In laminar flow ($Re<2300$), no radial mixing occurs, and the transfer of the solute from the round tube wall into the fluid stream is solely by molecular diffusion. For the case of a normal parabolic gradient, the analytical solution was presented by Sherwood *et al.*[9] When $C_L=0$ at the inlet, the average concentration over the cross section of the tube at the outlet, $(\overline{C_L})_{out}$ [mol/cm³], can be written as

$$1-\frac{(\overline{C_L})_{out}}{C_L^*}=0.819e^{-14.6272b}+0.0976e^{-89.22b}+0.0315e^{-212.2b} \quad (12)$$

where $b=D_L z_t/d^2u_0$; C_L^* [mol/cm^3] is the concentration of the solute at the wall surface, D_L[cm^2/s] is the molecular diffusivity of the solute, d [cm] is the diameter of the round tube and u_0 [cm/s] is the superficial velocity of the liquid. For the round tube, the mass transfer coefficient k_L based on the film theory can be written as (with $C_L=0$ at the inlet)

$$k_L=\frac{Q_L}{\pi z_t d}\ln\left\{1-\frac{(\overline{C_L})_{out}}{C_L^*}\right\}^{-1} \quad (13)$$

The calculated value for k_L obtained by substituting eq. (12) into eq. (13) is shown in Fig. 5. Our results are about threefold larger than those from eq. (13). This difference is too large to be explainable by uncertainties in D_L or other physical properties.

The main reason for the difference is considered to be the disturbance in the liquid, which is produced by the wave motion of the membrane resulting from the weak pulsation caused by the tube pump used in our experiment, and also by the zig-zag structure of the groove. This results in larger values of k_L than those of laminar flow. The k_L for turbulent flow in a round tube is shown as a line on the right-hand side in Fig. 5, as estimated from the correlation of Linton *et al.*[10] Other reasons for the difference may be the differences in the geometry of the cross section and the direction of diffusion. In the case of a round tube, the solute diffuses from the whole circumference (wall) toward the center. But, in our case, it diffuses from one side (membrane) toward the opposite side (wall). Thus, the concentration gradient may be larger for our configuration than for a circle. This would result in a larger k_L.

The curves in Fig. 3 were estimated by using the values of $(k_M)_0$, k_P and k_L (eq. (11)). They agree well with the experimental data. These values were used to analyze the rate data on the oxidation of glucose in the membrane reactor.

II. Oxidation of Glucose in the Membrane Reactor

(a) Intrinsic Kinetics———The rate of this enzyme reaction is well expressed by the following Michaelis-Menten equation, and both the maximum velocity, V_{max}[mol/(s·unit)], and the Michaelis constant, K_m [mol/cm^3], are proportional to the concentration of oxygen in the liquid, C_i [mol/cm^3].[5,6]

$$r=\frac{V_{max}C_E C_S}{C_S+K_m}=\frac{kC_E C_S C_i}{C_S+K_m' C_i} \quad (14)$$

where r[mol/(cm^3·s)] is the intrinsic rate of reaction, C_E[unit/cm^3] and C_S [mol/cm^3] are the concentrations of glucose oxidase and glucose in the liquid, respectively, and k and K_m' are proportionality constants.

To determine k and K_m', experiments were performed in the gas-liquid stirred tank reactor in 0.1 M acetate buffer solution (pH 5.5) at 20°C. The procedure was the same as reported in the previous paper.[6] The Lineweaver-Burk plots gave the values of $k=1.0\times10^{-2}$ [cm^3/(s·unit)] and $K_m'=60$ [−].

(b) Mass Balance Equation for Oxygen———Since the concentration of oxygen in the liquid is low (Table II), the concentration of glucose can be considered uniform throughout the membrane reactor and the limiting reactant is oxygen. In the steady state, the mass transfer rates for oxygen through the gas- and liquid-side membranes per unit axial length, N_G [mol/(cm·s)], and N_L [mol/(cm·s)], can be expressed as

$$N_G=(k_M)_G a(C_G-C_O) \quad (15)$$

$$N_L=-Q_L\frac{\partial C_L}{\partial z}_i=k_L a(C_L-C_M)=(k_M)_L a(C_M-C_D) \quad (16)$$

where $(k_M)_G$ [cm/s] and $(k_M)_L$ [cm/s] are the permeation coefficients for the gas- and liquid-

side membranes, and C_O [mol/cm^3] and C_D [mol/cm^3] are the concentrations of oxygen in the enzyme solution at the gas- and liquid-side membrane surfaces, respectively (see Fig. 6).

The global rate of absorption (reaction) in the reactor, R[mol/s], can be expressed as

$$R=\int_0^{z_t}(N_G+N_L)\,\partial z \tag{17}$$

Glucose solution saturated with oxygen at 1 atm is introduced into the reactor, so that

$$C_L=1/H \qquad \text{at } z=0 \tag{18}$$

For the mass balance equation for oxygen in the enzyme solution, two models can be considered; one is the case in which the enzyme solution is stagnant, *i.e.*, "the stagnant model," and the other is the case in which the enzyme solution is perfectly mixed in the w direction perpendicular to the z direction, *i.e.*, "the mixing model." The oxygen concentration profiles for both models are illustrated in Fig. 6.

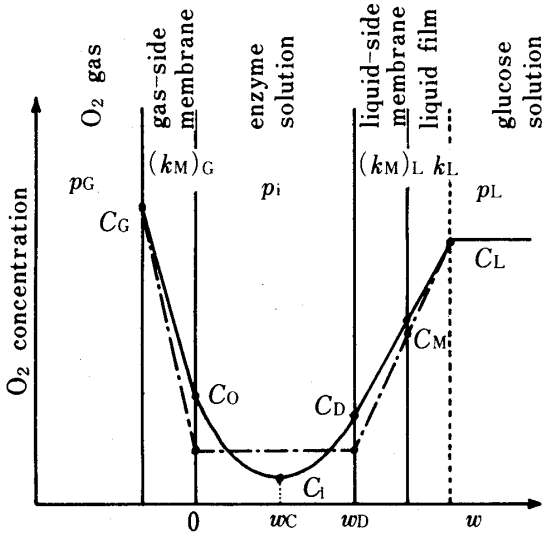

Fig. 6. Profiles of Oxygen Concentration in the Membrane Reactor
——— , stagnant model; – – – – , mixing model.

In the case of the stagnant model, the mass balance equation in the enzyme solution can be expressed by eq. (19) with the boundary conditions (20);

$$D_L\frac{\partial^2 C_i}{\partial w^2}=r \tag{19}$$

$$\left.\begin{aligned} -D_L\frac{\partial C_i}{\partial w}&=(k_M)_G(C_G-C_O) && \text{at } w=0\\ \frac{\partial C_i}{\partial w}&=0 && \text{at } w=w_C\\ -D_L\frac{\partial C_i}{\partial w}&=(k_M)_L(C_D-C_M) && \text{at } w=w_D \end{aligned}\right\} \tag{20}$$

where w_D [cm] is the thickness of the enzyme solution, and w_C [cm] is the position where the concentration gradient is zero (see Fig. 6).

For the mixing model, there is no concentration gradient for oxygen. Thus, the concentration of oxygen in the enzyme solution, C_i [mol/cm^3], is uniform in the w direction, and $C_i=C_D=C_O$. Then, the mass balance equation for oxygen can be simplified to

$$(k_M)_G(C_G-C_i)+(k_M)_L(C_M-C_i)=r\cdot w_D \tag{21}$$

As mentioned already, the membrane permeation coefficient depends on the pressure difference between the two sides of a sheet of membrane, that is, the distance z. However, it is very difficult to estimate the pressure of the enzyme solution at z. Furthermore, the reaction system becomes very complex if the pressure of the flowing liquid at any z is considered. Here, the pressure of each liquid will be assumed to be expressed as the average as follows:

$$\left.\begin{aligned} \overline{p_i}&=(p_G+\overline{p_L})/2\\ \overline{p_L}&=\{(p_L)_{in}+(p_L)_{out}\}/2 \end{aligned}\right\} \tag{22}$$

where $\overline{p_i}$ [atm] and $\overline{p_L}$ [atm] are the average pressures of enzyme solution and the flowing liquid, respectively. Using a relation similar to eq. (3), eq. (22) gives the average permeation coefficient as follows;

$$\left.\begin{aligned}(\overline{k_M})_G &= (k_M)_0 + k_P(p_G - \overline{p_i}) = (k_M)_0 + k_P(p_G - \overline{p_L})/2 \\ (\overline{k_M})_L &= (k_M)_0 + k_P(\overline{p_L} - \overline{p_i}) = (k_M)_0 - k_P(p_G - \overline{p_L})/2\end{aligned}\right\} \quad (23)$$

(c) Global Rate of Reaction——As described in the experimental section II(a), the amounts of oxygen absorbed through the gas- and liquid-side membranes were measured in the steady state. The experimental results are shown in Fig. 7. Clearly, the global rate of absorption (reaction) depends on both Q_L and p_G. In particular, the rate increases with p_G. It is also clear that, at higher p_G and lower Q_L, the transfer of oxygen through the gas-side membrane contributes greatly to the global rate. It is interesting that the rate through the gas-side membrane decreases with increase in Q_L, and that, at lower p_G (1.00 atm) and higher Q_L (1.02 cm^3/s), the rate for the liquid-side membrane is larger than that for the gas-side one.

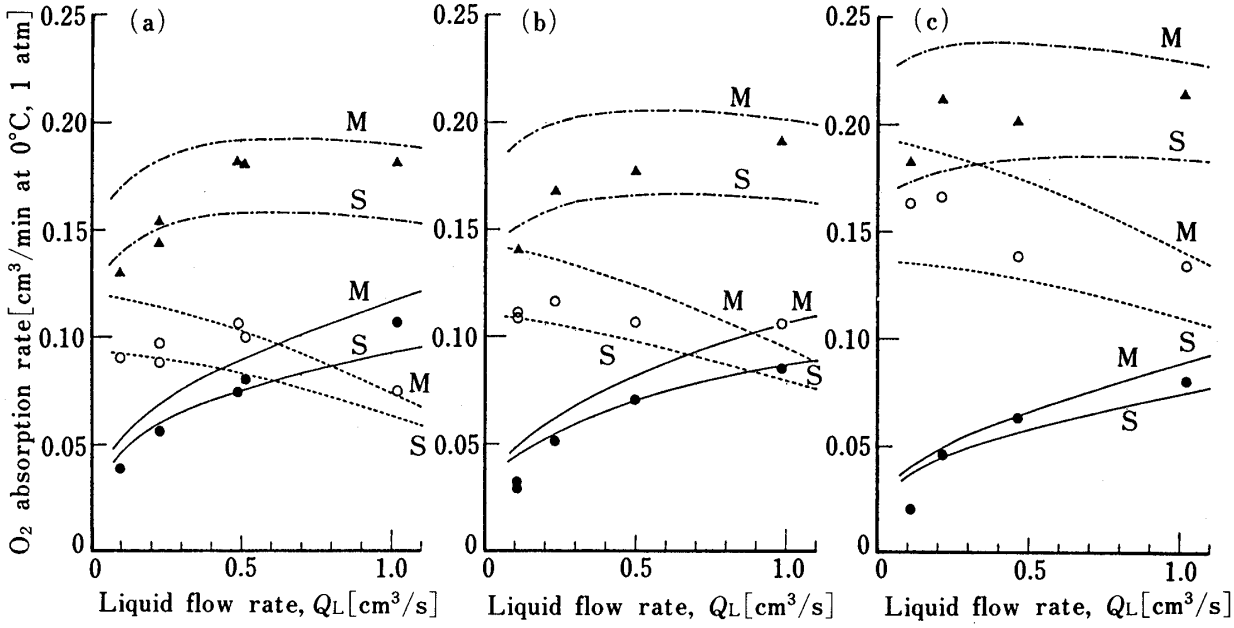

Fig. 7. Oxygen Absorption Rate in the Membrane Reactor at P_G=1.00 (a), 1.05 (b), and 1.15 (c) [atm]
Data : ○, gas-side ; ●, liquid-side ; ▲, total. Calculated curve : ------, gas-side ; ——, liquid-side ; —·—, total. Model : S, stagnant; M, mixing.

These results can be compared with the theoretical curves evaluated from the equations given in II(a) and II(b). For the stagnant model, the system equations (14) to (17) and (19) are used with the appropriate initial condition (eq. (18)) and boundary conditions (eq. (20)). For the mixing model, equations (19) and (20) are replaced by eq. (21). Because of difficulties in getting an analytical solution, these equations were integrated numerically. In this integration, the average values (eq. (23)) are used instead of the values of $(k_M)_G$ and $(k_M)_L$ in eqs. (15), (16), (20) and (21).

The curves obtained are shown in Fig. 7. The experimental results are, on the whole, situated between the curves for the two models, and are in good agreement with the stagnant model in the lower region of Q_L. On the contrary, the results are in good agreement with the mixing model in the higher region of Q_L. This tendency can be well explained by considering that, with increase in Q_L, the enzyme solution is well mixed in the w direction by the wave motion of the membrane.

Some additional factors affecting the global rate of reaction should be considered. For both models, the calculations were done by giving arbitrary values to the parameters C_E, w_D $(\overline{k_M})_G$ and $(\overline{k_M})_L$. The results are shown in Table III. The other conditions were kept constant and are given in the footnote.

TABLE III. Calculated Absorption Rate of Oxygen in the Immobilized Enzyme Membrane Reactor[a)]

C_E [unit/cm^3]	w_D [cm]	$(\overline{k_M})_G \times 10^3$ [cm/s]	$(\overline{k_M})_L \times 10^3$ [cm/s]	Oxygen absorption rate [cm^3/min at 0°C, 1 atm]					
				Mixing model			Stagnant model		
				Gas-side	Liquid-side	Total	Gas-side	Liquid-side	Total
34.6	0.117	0.777	0.785	0.1236	0.0818	0.2054	0.0971	0.0697	0.1668
34.6	0.117	2.5	0.785	0.3807	0.0781	0.4588	0.1977	0.0697	0.2673
34.6	0.117	0.777	2.5	0.1222	0.1527	0.2749	0.0971	0.1129	0.2100
34.6	0.117	2.5	2.5	0.3762	0.1457	0.5219	0.1977	0.1129	0.3106
34.6	0.05	0.777	0.785	0.1183	0.0781	0.1964	0.0971	0.0696	0.1667
80.7	0.05	0.777	0.785	0.1236	0.0818	0.2054	0.1062	0.0743	0.1805
80.7	0.117	0.777	0.785	0.1260	0.0834	0.2094	0.1062	0.0743	0.1805

a) For z_t=178.8 cm, a=0.48 cm, $(C_L)_m$=1.36×10^{-6} mol/cm^3, k=1.0×10^{-2} cm^3/(s·unit), K_m'=60, C_S=1.0×10^{-4} mol/cm^3, D_L=2.0×10^{-5} cm^2/s, p_G=1.05 atm, Q_L=0.50 cm^3/s, and k_L=2.03×10^{-3} cm/s.

The parameter values in the first line are the actual ones for one experimental run. The rates of oxygen absorption in this line are compared with those for the other conditions in Table III (lines 2 to 7). In the last three lines where the values of C_E and/or w_D are roughly doubled or halved, the rates are nearly the same as those in the first line. This can be easily understood because the rate is substantially controlled by the mass transfer of oxygen through both the membranes and the liquid film. In contrast, in the second to fourth lines where the values of $(\overline{k_M})_G$ and/or $(\overline{k_M})_L$ are changed, the rates change greatly from those in the first line, but the contributions of $(\overline{k_M})_G$ and $(\overline{k_M})_L$ to the rates are different. For example, for the mixing model, the increase in $(\overline{k_M})_G$ from 0.777 to 2.5 [cm/s] causes an increase in the total rate from 0.2054 to 0.4588 [cm^3/min] (more than 2 times). On the other hand, the increase in $(\overline{k_M})_L$ from 0.785 to 2.5 [cm/s] causes an increase from 0.2054 to 0.2749 [cm^3/s] (about 1.3 times). The same tendency can be seen for the stagnant model, though the increase in the total rate is not as large as with the mixing model.

These results indicate that the mass transfer through the gas-side membrane is the most important factor for the global rate of reaction, followed by the mass transfer through the liquid-side membrane and the liquid film. In other words, to improve the efficiency of such a membrane reactor as used in this study, it is necessary to decrease the permeation resistance of the gas-side membrane,as well as the liquid-side membrane.

As regards the reactor efficiency, the liquid flow rate and the gas pressure should be taken into consideration. As shown in Fig. 7, the total rate of absorption, that is, the global rate of reaction does not change as much as might be expected in the higher region of Q_L. Certainly the increase in Q_L increases the transfer rate of oxygen through the liquid side, mainly due to the increase in the liquid-to-membrane mass transfer coefficient which is proportional to the 0.56th power of Q_L (see eq. (11)). However, the transfer rate through the gas side decreases with increasing Q_L. This is because the pressure drop of the flowing liquid is proportional to the second power of Q_L. Therefore, the pressure difference between the gas side and the liquid side decreases, resulting in a decrease in the gas-side membrane permeation coefficient (see eq. (23)). As a whole, the liquid flow rate does not greatly influence the global rate of reaction. However, an increase of gas pressure improves the reactor efficiency. This is because the gas-side membrane permeation coefficient is considerably dependent on the gas pressure, as described in I(c).

Conclusions

The oxidation of glucose to gluconic acid by glucose oxidase was carried out in a membrane reactor which consisted of three sections; a gas-side section to which the oxygen gas was supplied, a liquid-side section where the glucose solution was flowing and a middle section of

enzyme solution. The sections were separated by two sheets of semipermeable membrane. This type of membrane reactor was found to be applicable to a gas-liquid two-phase enzyme reaction. Under conditions where the mass transfer of oxygen was important, the global rate of reaction was influenced mainly by the oxygen pressure applied to the gas side, and partly by the liquid flow rate. It was found from numerical calculations that the enzyme solution was stagnant at low liquid flow rates and moved in response to the wave motion of the membrane at high liquid flow rates. To improve the reactor efficiency, a means to decrease the membrane permeation resistance is required; of course, considerations of the physical and chemical properties of the membrane, such as strength, molecular weight cut-off, resistance to chemicals, innocuousness to enzymes, *etc.*, must also taken into account.

References and Notes

1) A part of this work was presented at the 102nd Annual Meeting of the Pharmaceutical Society of Japan, Osaka-shi, Apr. 1982.
2) O.R. Zaborsky, "Immobilized Enzymes," CRC Press, Cleveland, Ohio, 1973; I. Chibata (ed.), "Koteika Koso," Kodansha Scientific, Tokyo, 1975; K. Mosbach (ed.), "Methods in Enzymolozy," Academic Press, New York, Vol. 44, 1976; I. Chibata, "Immobilized Enzymes," Kodansha Ltd., Tokyo, 1978; S. Fukui, I. Chibata, and S. Suzuki (eds.), "Koso Kogaku," Tokyo Kagaku Dozin, Tokyo, 1981, p. 157.
3) A. Azhar and M.K. Hamdy, *Biotechnol. Bioeng.*, **23,** 1297 (1981); W.D. Deeslie and M. Cheryan, *ibid.*, **23,** 2257 (1981); *idem, ibid.*, **24,** 69 (1982); S. Furusaki and T. Miyauchi, *J. Chem. Eng. Japan,* **14,** 479 (1981).
4) F. Hsieh, B. Davidson, and W.R. Vieth, *J. Appl. Chem. Biotechnol.*, **26,** 631 (1976); H. Kitano, S. Yoshijima, S. Hotogi, and N. Ise, *Biotechnol. Bioeng.*, **22,** 2633 (1980); H. Kitano, S. Yoshijima, and N. Ise, *ibid.*, **22,** 2643 (1980); J.M. Engasser, J. Caumon, and A. Marc, *Chem. Eng. Sci.*, **35,** 99 (1980); H. Kataoka, T. Saigusa, S. Mukataka, and J. Takahashi, *J. Ferment. Technol.*, **58,** 431 (1980); D.E. Kohlway and M. Cheryan, *Enzyme. Microb. Technol.*, **3,** 64 (1981).
5) T. Tsukamoto, S. Morita, and J. Okada, *Chem. Pharm. Bull.*, **30,** 1539 (1982).
6) T. Tsukamoto, S. Morita, and J. Okada, *Chem. Pharm. Bull.*, **30,** 782 (1982).
7) Q.H. Gibson, B.E.P. Swoboda, and V. Massey, *J. Biol. Chem.*, **239,** 3927 (1964); S. Nakamura and Y. Ogura, *J. Biochem.* (Tokyo), **63,** 308 (1968); Y.K. Cho and J.E. Bailey, *Biotechnol. Bioeng.*, **19,** 185 (1977).
8) S. Furusaki, T. Kojima, and T. Miyauchi, *J. Chem. Eng. Japan.*, **10,** 233 (1977); S. Katoh, T. Yanagida, and E. Sada, *ibid.*, **11,** 143 (1978).
9) T.K. Sherwood, R.L. Pigford, and C.R. Wilke, "Mass Transfer," McGraw-Hill, New York, 1975, p. 83.
10) W.H. Linton and T.K. Sherwood, *Chem. Eng. Progr.*, **46,** 258 (1950).
11) D.M. Himmelblau, *Chem. Rev.*, **64,** 527 (1964).